EFDA–JET–PR(10)66

T.W. Versloot, R. Sartori, F. Rimini, P.C. de Vries, G. Saibene, V. Parail, M.N.A. Beurskens, A. Boboc, R. Budny, K. Crombé, E. de la Luna, F. Durodie, T. Eich, C. Giroud, V. Kiptily, T. Johnson, P. Mantica, M-L Mayoral, D.C. McDonald, I. Monakhov, M.F.F. Nave, I. Voitsekhovitch, K-D Zastrow and JET EFDA contributors and JET EFDA contributors

Comparison Between Dominant NBI and Dominant IC Heated ELMy H-mode Discharges in JET

Comparison Between Dominant NBI and Dominant IC Heated ELMy H-mode Discharges in JET

T.W. Versloot[1], R. Sartori[2], F. Rimini[3], P.C. de Vries[1], G. Saibene[2], V. Parail[4], M.N.A. Beurskens[4], A. Boboc[4], R. Budny[5], K. Crombé[6], E. de la Luna[7], F. Durodie[8], T. Eich[9], C. Giroud[4], V. Kiptily[4], T. Johnson[10], P. Mantica[1], M-L Mayoral[4], D.C. McDonald[4], I. Monakhov[4], M.F.F. Nave[12], I. Voitsekhovitch[4], K-D Zastrow[4] and JET EFDA contributors*

JET-EFDA, Culham Science Centre, OX14 3DB, Abingdon, UK

[1]FOM Institute Rijnhuizen, Association EURATOM-FOM, Nieuwegein, The Netherlands
[2]Fusion For Energy Joint Undertaking, Josep Pla 2, 08019, Barcelona, Spain
[3]JET-EFDA Close Support Unit, , Culham Science Centre, OX14 3DB, Abingdon, OXON, UK
[4]EURATOM-CCFE Fusion Association, Culham Science Centre, OX14 3DB, Abingdon, OXON, UK
[5]Princeton Plasma Physics Laboratory, Princeton, New Jersey, 08543, USA
[6]Department of Applied Physics, Ghent University, Belgium
[7]Laboratorio Nacional de Fusión, Asociación EURATOM-CIEMAT, Madrid, Spain
[8]Association Euratom-Belgian State, ERM/KMS, TEC Partners, Brussels, Belgium
[9]Max-Planck-Institut für Plasmaphysik, Boltzmannstrasse 2, D-85748, Garching, Germany
[10]Uppsala University, Association EURATOM-VR, Uppsala, Sweden
[11]Istituto di Fisica del Plasma 'P. Caldirola', Associazione Euratom-ENEA-CNR, Milano, Italy
[12]Associação EURATOM-IST, Instituto de Plasmas i Fusão Nuclear, 1049-001 Lisbon, Portugal
** See annex of F. Romanelli et al, "Overview of JET Results",*
(23rd IAEA Fusion Energy Conference, Daejon, Republic of Korea (2010)).

Preprint of Paper to be submitted for publication in
Nuclear Fusion

ABSTRACT.
The experiment described in this paper is aimed at characterization of ELMy H-mode discharges with varying momentum input, rotation, power deposition profiles and ion to electron heating ratio obtained by varying the proportion between Ion Cyclotron (IC) and Neutral Beam (NB) heating. The motivation for the experiment was to verify if the basic confinement and transport properties of the baseline ITER H-mode are robust to these changes, and similar to those derived mostly from dominant NB heated H-modes. No significant difference in the density and temperature profiles or in the global confinement were found. Although ion temperature profiles were seen to be globally stiff, some variation of stiffness was obtained in the experiment by varying the deposition profiles, but not one that could significantly affect the profiles in terms of global confinement. This analysis shows the thermal plasma energy confinement enhancement factor to be independent of the heating mix, for the range of conditions explored. Moreover, the response of the global confinement to changes in density and power were also independent of heating mix, and were reflecting the changes in the pedestal, which is in agreement with globally stiff profiles. Consistently, the pedestal characteristics (pressure and width) and their dependences on global parameters such as density and power were the same during NB only or with predominant IC heating.

1. INTRODUCTION

Extrapolations from present day machines to the ITER Q = 10 inductive standard scenario are predominantly based on ELMy H-modes heated by co-current Neutral Beam (NB) injection, yielding a power deposition that is off-axis and mainly directed towards the ions [1,2]. In ITER auxiliary heating is mainly on-axis and predominantly directed towards electrons while the standard Deuterium-Tritium scenario will be dominated by on-axis α-particle heating. The comparison of H-modes with predominant positive NB or predominant Ion Cyclotron (IC) heating can help therefore to confirm the prediction for ITER, in particular with respect to the pedestal behaviour [3] and the role of toroidal momentum input and fuelling [4,5]. Previous studies at JET suggested that confinement times depended on rotation, although the difficulty was to properly decouple power and torque [6]. Input power and torque are decoupled in H-modes with predominant IC. In JET H-modes at medium/high plasma current and density, the NB heating is deposited off axis, while IC can provide central electron heating, similar to ITER [7].

Previous experiments [8, 9, 10, 11] comparing predominantly IC and NB heated H-modes consistently reported no difference in energy confinement enhancement factor, H_{98}, or even an increase (<10%) in H_{98} with IC. The latter was attributed to more peaked electron temperature profiles due to more central power deposition with IC. Similarly, the H_{98}-factor did not vary significantly with T_i/T_e and the density profile shape in Hybrid scenarios with strong central IC in ASDEX Upgrade [12]. On the other hand, balanced beam experiments in DIIID [13, 14] show a decrease in H_{98} with low torque, while improved performance could be obtained with combined EC/IC heated discharges in ASDEX, although in the latter case only when significant NB heating was still applied [15].

The JET results in sawtooth-free H-mode phases, showed a tendency of electron temperature profiles to achieve invariance once the critical inverse gradient length threshold was exceeded, when performing an electron heat flux scan by using on- and off-axis dominant IC [11]. A detailed transport analysis in [16] showed a significant effect of rotation on the stiffness of the ion temperature profiles in the inner half of the plasma. As part of that analysis, NB and IC heated H-modes were also compared, concluding that the modest variation in T_i-profiles was due to the small variation of the normalised core heat flux when applying NB compared to IC, deriving from the less localised power deposition of NB at constant total power.

In these previous studies, the analysis of the pedestal behaviour is either missing or limited. Pressure pedestal analysis at JET [9, 10, 17] indicated indirectly that poloidal Larmor radius of the fast particles lost to the edge could determine the width of the pedestal pressure, p_{ped}. It was later shown, with the same indirect pedestal pressure analysis [8] but in a more extensive study, where long pulse high q_{95} discharges with IC and NBI heating were compared at the same density, that the pedestal width did not strongly depend on the fast particles Larmor radius (see also Ref. [3]). Ref. [8] finds similar ELM frequency, f_{ELM}, and p_{ped}, for IC and NB H-modes, while results from [9] show higher f_{ELM} and lower p_{ped} with IC.

The limited number of IC dominated Type I ELMy H-modes in the JET databases is due to the difficulties in coupling IC power with these ELMs. The experiment described in this paper is aimed at comparing Type I ELMy H-modes with dominant IC and dominant NB heating in a relevant JET H-mode operational space, i.e. in a range of plasma parameters that are comparable to the bulk of JET data for confinement, pedestal and ELM studies. This experiment was made possible by the availability of the ITER relevant ELM resilient systems (3dB and conjugate-T) installed in the JET A2 antenna and of the new JET ITER like (ILA) antenna [18]. The new JET High Resolution Thomson Scattering (HRTS) was used to provide pedestal data (n_e,T_e) that was not available in previous experiments.

This paper is outlined as follows: first the experimental strategy is presented in section 2 followed by the discussion of the general global properties obtained in both NB dominated and IC dominated discharges in section 3. The results of a more detailed study of the confinement and core transport of a set of direct comparison discharges with NB and with predominant IC heating, based on modelling results from JETTO, are presented and discussed in section 4. The pedestal pressure and width characteristics for NB and IC dominated discharges and their trends with global parameters are discussed in section 5. Section 6 summarises the main conclusions and their relevance for ITER.

2. EXPERIMENTS

The scope of this experiment in JET was to compare both pedestal and ELMs, as well as core confinement and transport of Type-I ELMy H-modes with IC and NB heating. The experiments were carried out in a relevant H-mode operational space in terms of plasma current, I_p (= 2.5MA), q_{95} (= 3.6) and density (= 60-70% of the Greenwald density, n_G). In order to maximise the coupled

IC power, H-minority heating at $B_t = 2.7T$ with 42MHz dipole phasing was used, allowing all the JET ELM-resilient systems, including the new ILA antenna [20], to be employed together. In addition, a standard low triangularity ($<\delta>\sim 0.25$) plasma configuration was chosen, as having a good coupling characteristics. Under these conditions, up to 9MW of IC power could be reliably coupled in a typical type-I ELMy H-mode. In all discharges, the H-mode is formed with NB injection only in the starting phase. After reaching an initial steady state, the NB was subsequently ramped down while simultaneously applying IC heating to achieve the requested IC heating fraction, $f_p = P_{IC}/(P_{NB}+P_{IC})$ and total input power. The duration of this ramp phase was approximately the same and independent of heating mix. The direct comparison between IC and NB is carried out once a new stationary condition (constant stored energy and density for several confinement times) is reached. This reason for this method is twofold. First, the density increase in H-mode with no IC heating phase is observed to be more stable due to reduced risk on long sawtooth periods, crashes and associated MHD. Secondly, it ensures similar starting references in both IC and NB discharges required for direct comparison. A range from NB only ($f_p = 0$) up to full IC ($f_p = 1$) H-modes was explored, albeit not all with the same total heating.

H-modes heated only by NB were compared to H-modes with 50:50 IC:NB, with a total loss power (P_{loss}) of ~16MW, which was about twice the L-H threshold power. Comparisons were also done at lower levels of total power, down to ~1.2 the L-H threshold power and with various fraction of IC heating up to 100% IC ($f_p = 1.0$). The bulk of the comparisons were performed at a line average density of ~65% of the Greenwald density, corresponding to $n_G \sim 5.7 \times 10^{19}\ m^{-3}$. This density is slightly higher than the natural density for NB H-modes with this plasma configuration, which is ~60% n_G. This was because some base level of external gas fuelling with D_2 and/or H_2, the latter for minority heating, was maintained in both NB and IC H-modes. The Hydrogen concentration, measured at the edge, was maintained to 4±0.5% for all H-modes, even for those with NB only. Furthermore, experiments were done at a higher density of (~70% of n_G) via increased D_2 gas fuelling. Since the NB system also provides particle fuelling, some IC comparison cases at constant power were carried out with the same fuelling rate used with NB. Finally, discharges with combined IC and NB heating up to P_{loss} of 24MW were achieved.

3. GENERAL RESULTS

The overall comparison of the confinement of H-modes with NB and with combined heating at different fractions of IC power, different levels of total power and different density shows that the thermal energy confinement enhancement factor ($H_{98(y)}$) does not depend on the heating mix, as seen in Fig.1. As usually found at JET, $H_{98(y)}$ decreases with increasing density [19]. Some further degradation of the energy confinement is seen when the total external heating power is reduced. This aspect is discussed in Section 5.

A more detailed comparison between H-modes heated by NB and by predominant IC was carried out by studying matching pairs of H-modes at similar density and power, but with a different heating mix. The divertor D_α traces of these pairs of H-modes with decreasing levels of total power are shown in Fig.2a for varying levels of IC ($f_p > 0$) and in Fig. 2b for matched NB heating only ($f_p = 0$). In the H-modes with combined IC and NB heating, the IC power was kept constant while decreasing the total power, therefore the IC proportion increases as the power decreases The IC proportion is 50% at 16MW total power and increases up to 100% IC at P_{loss}~9MW (see also Fig.2a). The IC fraction and loss power were therefore not independently varied during the experiment.

No obvious correlation between ELM frequency (f_{ELM}) and external heating mix is found. In fact, f_{ELM} is lower during NB heating only at 16MW in comparison to the combined heating case, but it is higher with NB at 13MW. Z_{eff} varies from 1.7 to 2.0 in all the pairs of H-modes of the comparison, apart from the NB only case with the highest loss power, where it reached a slightly higher value of ~2.5. In order to maintain the same density, a three times higher gas rate, was necessary in the case of IC+NB than with NB heating only in the matched pair of discharges at 16MW. The H-mode at $f_p = 0.5$ was repeated with the same lower gas fuelling as in the comparable NB only plasma, and in this case the density decreased from 60% to 45% n_G. For all the other comparison pairs at lower power (lower NB) instead, similar density was obtained with the same gas flow of $1.5{\times}10^{22}$ electrons/s. Common to all the pairs that reach the same density is the fact that an approximate fuelling balance, carried out assuming a fuelling efficiency of 0.9 for NB fuelling and of 0.1 for gas fuelling, shows that the difference between the total external fuelling flux in the IC and NB plasmas is $\sim10^{20}\ s^{-1}$, much lower than the recycling flux [20] of $\sim10^{22}\ s^{-1}$. ELM loss analysis shows that the ELM power fluxes (calculated as $<\Delta W_{ELM}> f_{ELM}$ in MW) are comparable in the IC and NB pairs, despite the difference in ELM frequency. Therefore it is not unreasonable to assume that also the ELM particle flux is similar. When lower density is obtained with IC, this seems to be predominantly due to lower external fuelling and not to changes in ELM particle losses. Figures 3a and 3b show the main plasma parameters for two comparison pairs with $f_p = 0.5$ at P_{loss}~16MW and with $f_p = 0.85$ at P_{loss}~11MW. As indicated by Fig.1, the differences in energy confinement enhancement factors within the pairs are at most 10% at similar density and not systematic. In fact at 16MW the NB H-mode has a higher $H_{98(y,2)}$, while at 11MW the IC dominated H-mode has a higher confinement enhancement factor.

4. TRANSPORT AND CONFINEMENT

Core density and temperature profiles with predominant IC or NB heating are similar for all the comparison pairs at similar density and power of figures 2a and 2b. This is shown in Fig.4 for both the H-mode with $f_p = 0.85$ (4a, 4b and 4c) and for the H-mode with $f_p = 0.5$ (4d, 4d and 4e). Some increase in the ion (T_i) and electron temperatures (T_e) profiles inside the sawtooth inversion radius, which corresponds to <20% of the plasma volume, is observed with predominant IC. In all these H-modes at relatively high density, the ion and electron temperature profile are similar although differences in the edge temperature offset the global temperature profile. The largest difference between T_e and T_i is less than 20% at the highest NB power of 16 MW, with no apparent correlation with f_p, P_{loss} or applied torque, T_φ. However, the reduction of the NB fraction, and hence T_φ, resulted in a significant drop in plasma toroidal rotation, ω_{tor}, as measured by Charge Exchange Recombination Spectroscopy (CXRS). Discharges with f_p>0.5 had approximately 5 times lower ω_{tor} in the core and ~10 times lower values in the edge compared to the NB only cases. The Mach number dropped from ~0.4 with NB heating to <0.1 at almost fully IC heating.

Interpretative transport analysis was carried out with the JETTO code for these two comparison pairs, with a power of 16MW and 50:50 IC:NB ($f_p = 0.5$) and a power of 11 MW with 85:15 ($f_p = 0.85$), respectively. The power deposition profiles were changed significantly from mainly off-axis with NB only to mainly on-axis in the case of predominant IC as shown in Fig 5a for $f_p = 0$ and $f_p = 0.85$ at 11MW. In fact, by changing the total power, the beam energy and, more importantly, the beam to IC proportion, the power deposition profiles were changed significantly during the experiment. For NB only heating, the fraction of power deposited inside $\rho = 0.5$ is typically of the order of 40% of the total power, increasing to 60% for $f_p = 0.5$ and in the case of $f_p = 0.85$ an extremely peaked power deposition is obtained with up to ~85% deposited inside mid-radius. To put this in perspective, the power deposition in the baseline Q = 10 ITER scenario (including α-particles) is predicted to have ~70% on the power deposited on ions and electrons within mid radius [2]. The power to ions and electrons also changed significantly with increasing IC fraction; at 50% IC heating approximately 14% more power was absorbed by ions while at 85% IC heating, the electrons received 40% more power. While in the comparison case of NB only, as shown in Fig.5b, the power was equally distributed over ions and electrons as well as broadly over the entire plasma profile. With an increase in direct electron heating, the exchange power from electron to ions also increases. This process is peaked at mid-radius (see also Fig.5a). Further towards the edge, a higher T_i compared to the local T_e then caused an exchange from ions to electrons.

The resulting effective ion and electron heat diffusivities for the same H-modes are shown in Fig. 5c. The larger core power deposition, as the IC fraction was increased, did not lead to a significant difference in the ion temperature profile, suggesting that these profiles are generally stiff. Indeed, the profiles of $\chi^{eff}{}_i$ and $\chi^{eff}{}_e$ increase in the plasma core and gradient region in the case of $f_p = 0.5$, while they are similar further outwards where the volume integrated heat fluxes from direct heating and thermal exchange become comparable.

Due to the decrease in torque with increasing IC fraction, the gradient in rotation is significantly reduced and the question arises if this has an impact on the stiffness of the ion temperature profile and the transport in general, as observed in in earlier JET experiments [16]. A trend is not directly visible in the ion temperature profiles shown in Fig.4. However, one has to be careful as the power deposition and heat fluxes also vary considerably between these plasmas. Hence in Fig.6, similarly as in Ref. [16], the normalised ion heat flux (q_{GB}) is plotted against the normalised inverse ion temperature gradient length, $R/L_{Ti} = (R/a)(1/T)dT_i/d\sqrt{\psi_{pol}}$. The data points are marked according to the total heating fraction (f_p) and the value of the local toroidal rotation gradient (ω) around $\rho \sim 0.4$+/-0.1. The location of the comparison cases as shown in Fig.2 are marked in full symbols with estimated error bars. Logically, the high rotation data is mostly populated by discharges with a low IC fraction ($f_p < 0.3$), while the high normalised heat flux region is populated by discharges with an increased IC fraction. In general a similar range in R/L_{Ti} values is obtained for all discharges. At high normalised ion heat flux ($q_{GB} > 5$) however, the area with a lower R/L_{Ti} is more populated by discharges with a lower rotation gradient, while the higher rotation cases tend to have larger R/L_{Ti}. A similar analysis done for data taken radially further outwards, suggest that the separation between the high and low rotation cases completely disappears.

The interpretation of these data is not unambiguous, in particular due to the relatively large error in the gradient data (up to 40%) as well as the spread in low rotation gradient data due to low levels of external torque. Nevertheless, these observations are consistent with the results shown in Ref. [16]. As the width and volume Jacobean of this low stiffness region are however small, no significant differences in the global confinement properties are observed (see also Fig.1). In addition, the above analysis does not separate the core plasma from the influence of the pedestal, which is known to play an important role in the global confinement of an ELMy H-mode [19, 21]. Note for example that both the normalised heat flux and value of R/L_{Ti} are smaller in the NB only case at 16MW compared to the H-mode at 11MW. This is partly due to the difference in power deposition but also due to differences in the temperature pedestal between these discharges.

5. PEDESTAL AND ELMS

The pedestal analysis was carried out using density and temperature profile data obtained by High Resolution Thompson Scattering (HRTS) and by Electron Cyclotron Emission (ECE) diagnostics for the temperature data, and further information on the density from the FIR interferometer. The comparison of the pairs of H-modes with NB and with combined heating shows that the pedestal pressure does not depend on the heating mix. This is illustrated in Fig.7 that shows the n_e-T_e diagram of all H-modes in this analysis at both low and high density and various heating fractions. Highlighted are the pairs of matched H-modes of Fig.2.

An average constant pressure line is drawn in Fig.7 (full line). In general, the points follow this constant pressure line as the density increases. However, the figure also shows that, independent of additional heating mix, a group of discharges deviates from the constant pressure towards lower pedestal temperature. These discharges show a decrease of H_{98} when the density is increased at constant power (see also Fig.1). This is due to two factors that take place either separately or combined. Firstly, the confinement time scaling predicts an increase of stored energy with density and hence a decrease in $H_{98(y,2)}$ even when both pedestal- and total stored energy remain constant in the experiment [1]. Secondly, a decrease of pedestal temperature with density stronger than $T \propto 1/n$, which is seen in JET mostly at low triangularity [19,21], produces a lower total stored energy.

It is therefore not surprising that H_{98} is seen to decrease with density here, even with approximately constant pressure. The clear decrease in the pedestal pressure in Fig.7., which is correlated with the decrease in $H_{98(y,2)}$ at almost constant density, is observed when the the loss power is reduced from

16MW to approximately 9MW as illustrated in Fig.8. This degradation of $p_{e,ped}$ with decreasing power, which occurs independent of heating mix, is due to a decrease of the pedestal temperature as illustrated in Fig.9 and is seen in both ECE and HRTS data. The decrease of pedestal temperature with power is also independent of heating mix. This effect could be specific of the low triangularity configuration used in this experiment, and related to the fact that, by decreasing the power, the margin above the threshold power was also decreased. Not only the pedestal pressure and its trends are similar with different heating mix, the pedestal temperature (and density) widths are found to be independent of heating mix, as shown in Fig. 9. Therefore the temperature and density pedestal widths are also independent of power.

Although the ELM frequency varies between H-modes with NBI and with predominant IC at the same power, this variation does not seem to be correlated with changes in the heating mix. Even if the ELM frequency, f_{ELM}, can be different, the comparison of the pairs of H-modes at the same total power and density, with NB and with dominant IC, shows that the power loss by the ELMs, $f_{ELM}\Delta W$ is the same. The power loss by the ELM is also seen to increase with power. In summary, the pedestal is similar in both IC and NB with similar trends. The variation of the H-factor observed reflects changes in the pedestal in both cases, as is normally seen in ELMy H-modes [1].

DISCUSSION AND CONCLUSION

The experiment described in this paper aimed to characterise ELMy H-mode for plasmas with varying momentum input, rotation, power deposition profiles and ion to electron heating ratio obtained by varying the external heating mix. The motivation was the verification that the basic plasma confinement properties of the baseline ITER $Q = 10$ H-mode scenario are similar to those derived from the large database of dominant NB heated H-modes, where heating is normally associated to large momentum input, the coupling between injected power and rotation, as well as with core fuelling.

The power deposition profiles varied from very peaked (~85% power inside $\rho = 0.5$) with predominant IC, to flat deposition for pure NB cases. The plasma toroidal rotation was varied by a factor of ~5 in the core and ~10 in the edge. Those variations did not produce any significant difference in the density and temperature profiles or in the global confinement. An analysis of the variations of the normalised ion temperature gradient length with normalised ion heat flux showed that in general ion temperature were stiff. Albeit a small variation in stiffness was found, dependent on the plasma rotation, similar as reported in [16]. However, these variations had no significant effect on the global confinement due to the finite volume. The impact of rotation of the ion temperature profile stiffness is also thought to be limited in the presence of large magnetic shear, such as in these discharges with fully developed q-profiles [22].

This analysis shows the thermal plasma energy confinement enhancement factor to be independent of the heating mix, for the range of conditions explored. Moreover, the response of the global confinement to changes in density and power, and the consequent variations of H_{98}, were also seen to be independent of heating mix. The H_{98} factor was seen to decrease with density, as normally seen in ELMy H-modes, and with power, at low power above the threshold power. These variations are mainly reflecting changes in the pedestal. The pedestal characteristics (pressure and width) and their dependences were found to be independent of heating mix. The differences in global confinement were mainly associated to changes in pedestal pressure (or temperature).

Finally, the range of the power deposition profile, ion to electron power deposition, core fuelling and momentum injection are inclusive of what is expected for the ITER baseline scenario. The results presented here indicate that the global confinement scaling at the basis of the ITER Q = 10 performance prediction is robust in spite of having being derived from a majority of plasma H-modes with high momentum input, prevalent ion heating and relatively flat deposition profiles.

ACKNOWLEDGEMENTS.

This work was supported by EURATOM and carried out within the framework of the European Fusion Development Agreement. The views and opinions expressed herein do not necessarily reflect those of the European Commission. The views expressed in this publication are the sole responsibility of the author and do not necessarily reflect the views of Fusion for Energy. Neither Fusion for Energy nor any person acting on behalf of Fusion for Energy is responsible for the use which might be made of the information in this publication.

REFERENCES

[1]. Doyle E.J. (Chair Transport Physics) 2007 Nuclear Fusion **47** S18
[2]. Wagner F. et al., 2010 Plasma Physics and Controlled Fusion **52** 124044
[3]. Maggi C.F. et al., 2007 Nuclear Fusion **47** 535
[4]. Halpern F.D. et al., 2008 Physics of Plasmas **15** 062505
[5]. Budny R.V. et al., 2009 Nuclear Fusion **49** 085008
[6]. de Vries P.C. et al., 2008 Nuclear Fusion **48** 065006
[7]. Noterdaeme J-M et al., 2003 Nuclear Fusion **43** 202
[8]. JET TEAM (prepared by F.G. Rimini and G. Saibene) 2002 Nuclear Fusion **42** 86
[9]. Lingertat J. et al., 1999 Journal Nuclear Materials **266** 124-130
[10]. Bhatnagar V.P. et al., 1999 Nuclear Fusion **39** 353
[11]. Suttrop W. et al., 2001 in the Proc. of the 28th EPS Conf. on Plasma Physics (Madeira, Portugal, 2001)
[12]. Stäbler A. et al., 2005 Nuclear Fusion **45** 617
[13]. Solomon W.M. et al., 2007 Plasma Physics and Controlled Fusion **49** B313
[14]. deGrassie J.S. 2009 Plasma Physics and Controlled Fusion **51** 124047
[15]. Sips A.C.C. et al., 2007 Nuclear Fusion **47** 1485
[16]. Mantica P. et al., 2009 Physical Review Letters **102** 175002
[17]. Parail V.V. et al., 1999 J. Nuclear Fusion **39** 369

[18]. Durodie F. et al., 2010 in the Proc. of the 23rd IAEA FEC (Daejeon, Korea, 2010)
[19]. Saibene G. et al., 1999 Nuclear Fusion 39 1133
[20]. Kallenbach A. et al., 2003 Nuclear Fusion **43** 573
[21]. Beurskens M.N.A et al., 2009 Plasma Physics and Controlled Fusion **51** 124051
[22]. Mantica P. et al., 2010 in the Proc. of the 23rd IAEA FEC (Daejeon, Korea, 2010)

Figure 1: Energy confinement enhancement factor versus normalised density n_e/n_G for H-modes with different heating fractions, $f_p = P_{IC}/(P_{IC} + P_{NB})$.

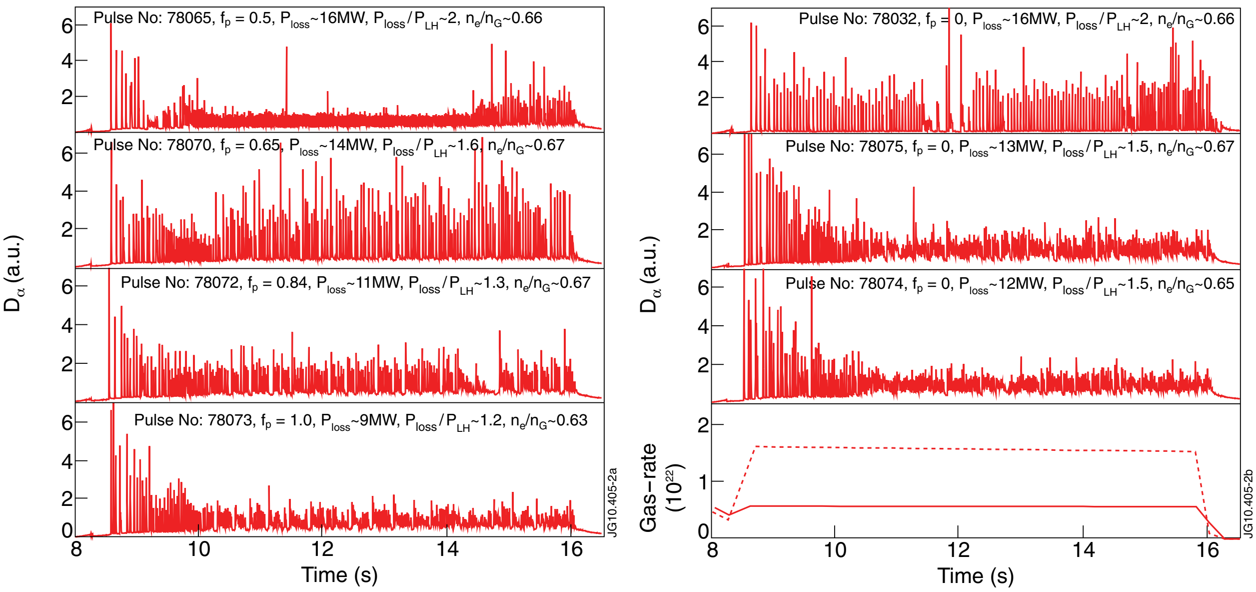

Figure 2: (a) Combined heating H-modes (IC and NB) with varying proportion of IC power (ranging from 50 to 100%) and varying total input power (from ~16MW to ~9MW). Corresponding comparison H-mode with NB only is shown on the right, apart from the 9MW case. (b) H-modes heated by NB only with varying total input power (from ~16MW to 12MW). The bottom time trace shows the two levels of gas fuelling (ϕ_{gas}) with the full line for the NB only at 16MW and the dashed line for all others as well as the comparisons at IC:NB mixture.

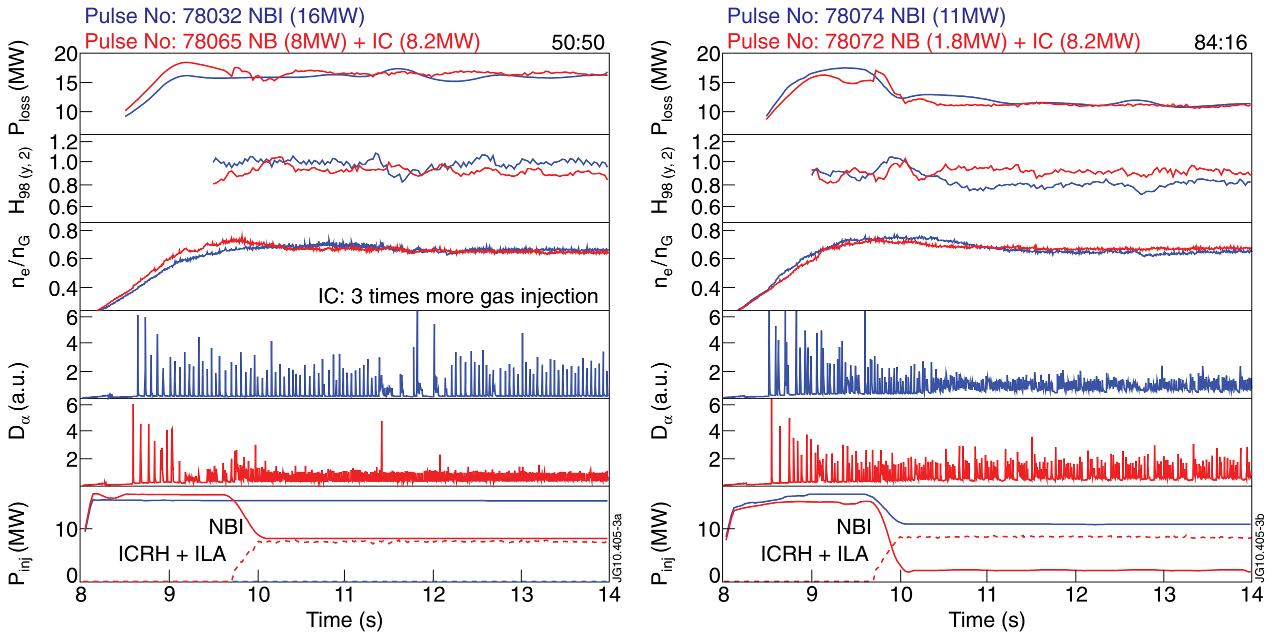

Figure 3: Time traces of the main plasma parameters. (a) For H-modes at 16MW with NB only (blue) and 50:50 IC:NB heating mix (red). (b) For H-modes at 11MW with NB only (blue) and with ~85:15 IC:NB heating mix (red).

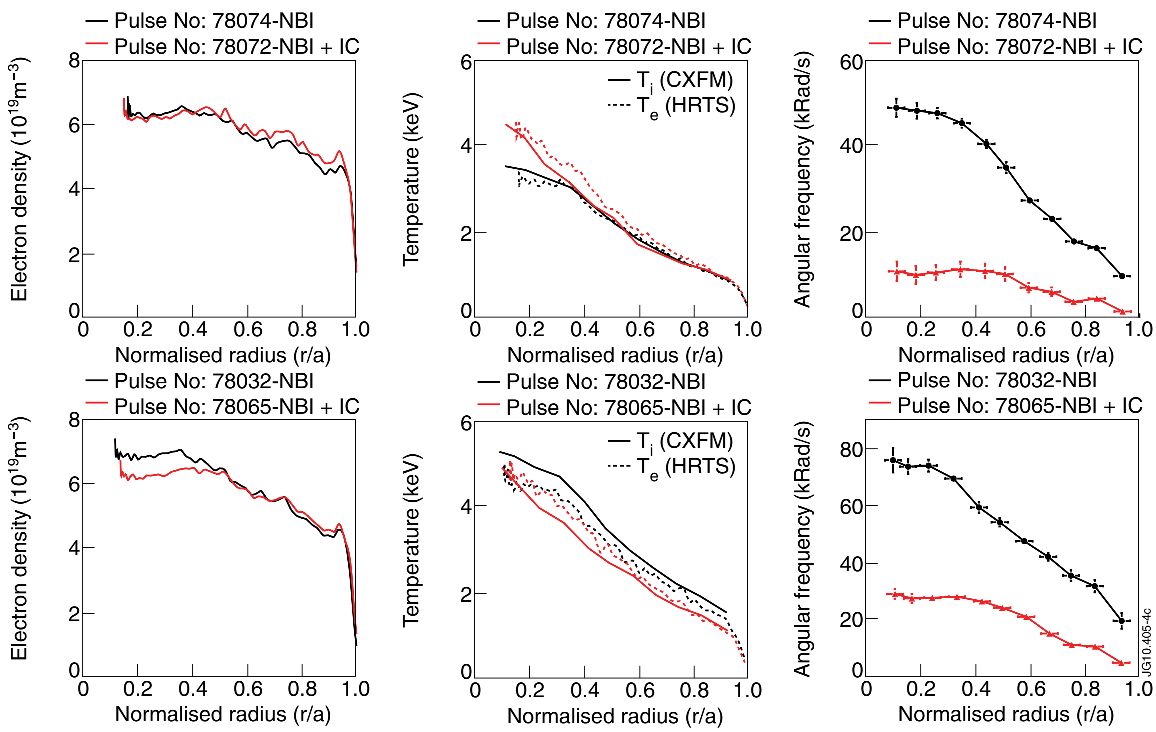

Figure 4: Several plasma profiles for both the 11MW (top row, f_p~0.5) and 16MW (bottom row, f_p~0.85) comparison cases with NB only (black) and IC:NB mixture (red). (left) Electron density profile from the HRTS diagnostic. (middle) Ion temperature (from CXRS) and electron temperature (from HRTS). (right) Angular frequency profile from CXRS. All profiles are time averaged over 1s in the steady-state phase.

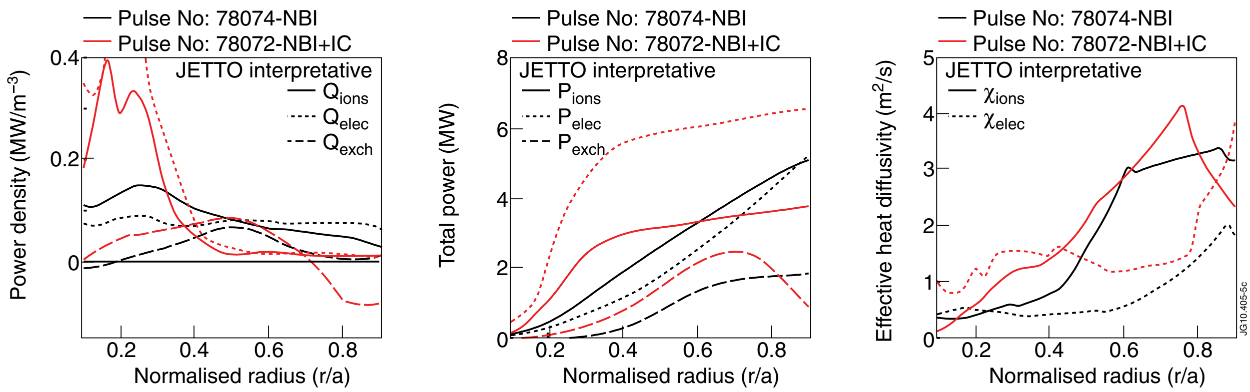

Figure 5: Interpretative transport results from JETTO for the NB only (black) and 85% IC (red) at 11MW with (a) Power density to the ions and electrons, and thermal exchange power from electrons to ions. (b) Integrated power to ions and electrons and (c) ion and electron effective heat diffusivity. Notice the higher power deposition in the plasma core when applying on-axis IC in comparison to off-axis NB heating.

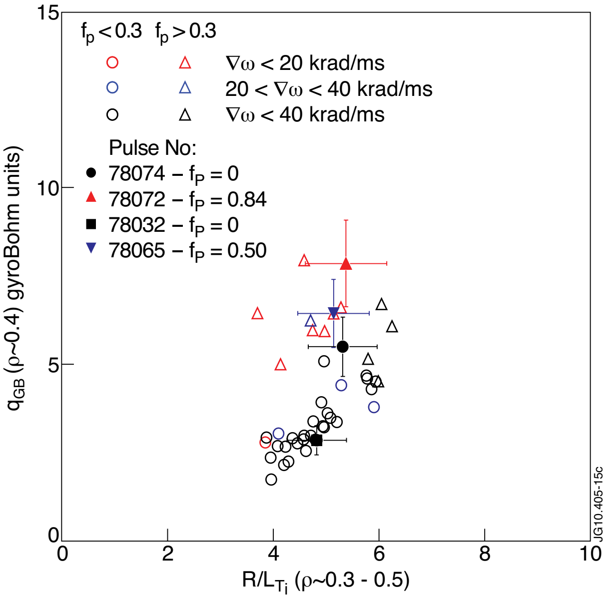

Figure 6: Normalised heat flux in Gyro-Bohm units versus normalised inverse gradient length of the ion temperature in a local gradient region around ρ ~ 0.4+/−0.1. The points are coloured to highlight two different levels of ∇ω (krad/ms), while the symbols differentiate the levels of total absorbed power and varying levels of IC heating (f_p). The comparison cases of Fig.2, are marked in full symbols with an estimate of error bars.

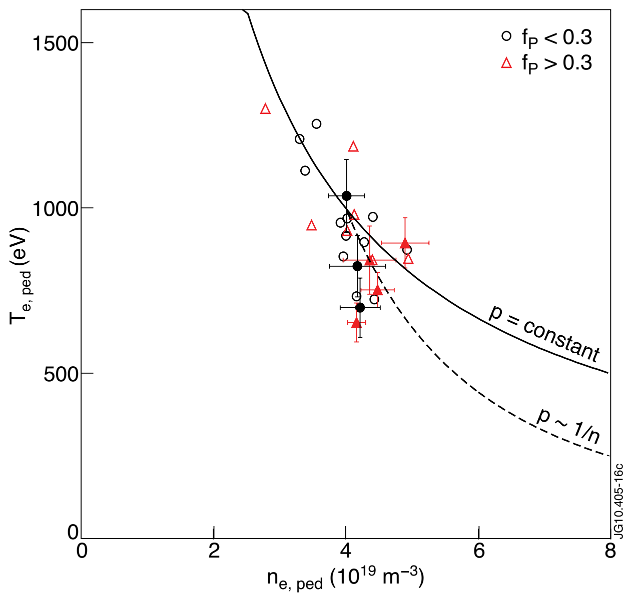

Figure 7: n_e-T_e diagram for H-mode discharges at varying levels of IC heating fraction, f_p. The comparison cases shown in Figure 2 are highlighted in full symbols for NB only (black) and dominant IC (red).

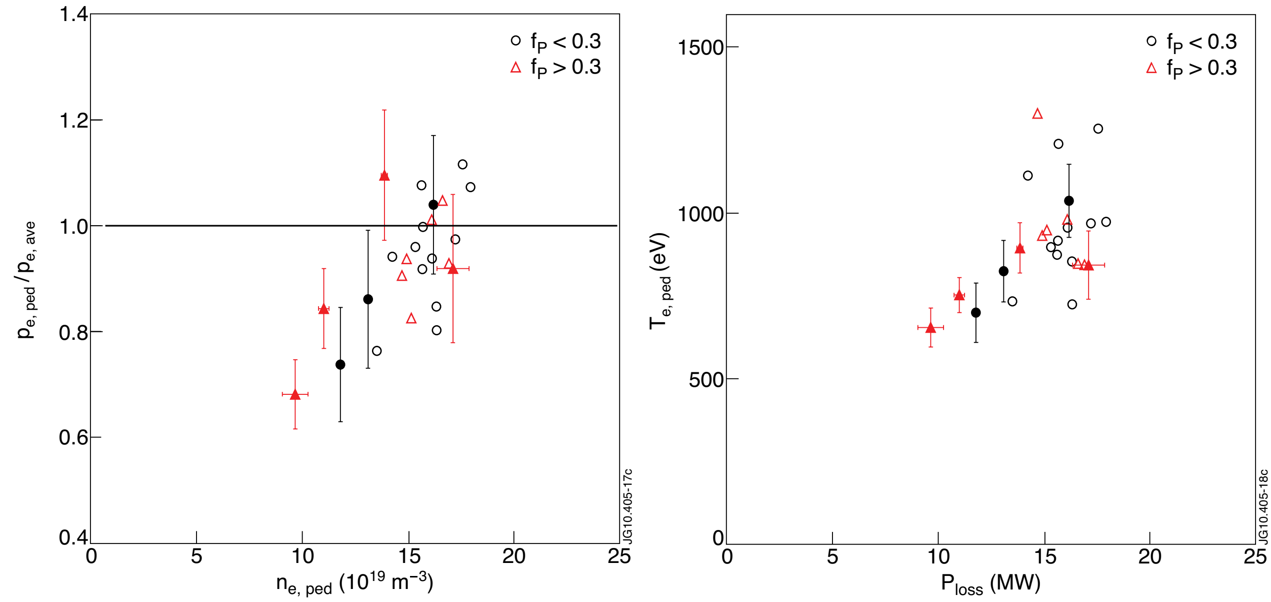

Figure 8: (a) Pedestal pressure normalised to the constant pressure value of Fig. 8, showing that the decrease in pedestal pressure is due to the decrease in input power. (b) Pedestal temperature versus loss power for all the pairs of comparable H-modes with NB (black) or predominant IC (red). The point at lowest temperature is the 100% IC which has no NB comparisons at the same power.

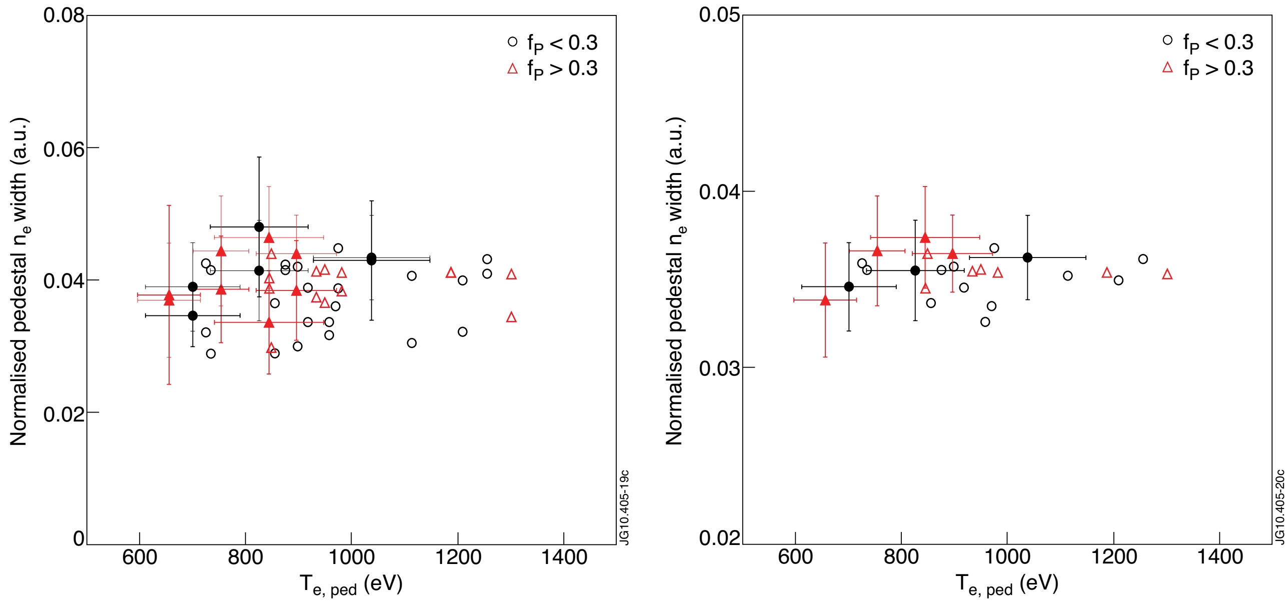

Figure 9: Normalised width of the electron temperature (a) and density pedestal (b) for all the discharges. The height of the pedestal parameters is determined here from the inter-ELM measured profiles.